Approach to make pNipam accessible for x-rays scattering experiments

Ewa Galasińska

Silesian University of Technology in Gleiwitz, Poland

Supervisor: Birgit Fischer & Martin A. Schroer

September 5, 2013

Abstract

This report summarizes my work as a DESY Summer Student in Hamburg. In my project colloidal suspension were studied by dynamic light scattering. The purposes of these experiments were to study the structure and dynamic of charged colloidal system made out of a thermoresponsive polymer at different temperature. To this end core-shell system consisting of Poly(N-isopropylacrylamide)/Silica Gel Hybrid were synthesized in water.

Contents

1 Introduction

This report serves to present the results of my work during my participation in the DESY Summer Student Program 2013. My project was focused on preparing colloidal samples and investigating them by means of dynamic light scattering techniques. The colloidal sample synthesized were core-shell particle made out of Silica/pNipam was synthesized.

PNipam is thermoresposive polymer that remains the leading substance for biomedical applications because of the sharpness of the transition temperature which is close to the body temperature. PNipam undergoes a reversible state transition; it switches from a hydrophilic, swollen state below its transition temperature (LCST ~ 32°C), to a hydrophobic, collapsed state above it. Concentrated systems cannot be studied by light scattering since they are turbid or opaque.
For these concentration multiple scattering occurs makes a directly interpreted of light scattering data impossible. However X-ray scattering techniques allow even for opaque system reliable results. For this a high electron density contrast is needed. Unfortunately pNipam consist almost of carbon and hydrogen which gives not a good contrast compared to water. In addition due to the high intense x-ray beam, beam damage occurs quite fast. In contrast to pNipam/Silica particle to be known to scatter x-rays strongly. Therefore we wanted to combine the properties of silica, as a good x-ray scatters with the thermoresponive behavior of pNipam and synthesized a silica/pNipam core shell system.

The development of this core shell materials will open up a new system to investigate by x-rays scattering methods.

2 Colloids especially silica, pNipam and core-shell particles

2.1 Colloidal System

Colloidal systems (also named as colloidal dispersion, colloidal suspension) are defined as a mixture of two substances. The dispersed phase is uniformly distributed within the dispersion medium (or dispersing medium). The dispersion medium or disposed phase may be a gas, liquid, or solid. In nature one can find a large variety like blood, milk, protein, smoke, dust. Colloids have the advantage that their time scales are lager and relaxation processes are much slower than that of molecular liquids which means that they can be studied using optical techniques like microscopy and dynamic light scattering [1].

The phase behavior of molecular systems can be studied in general by using colloidal suspensions. There are two types of stabilization for colloidal particles.

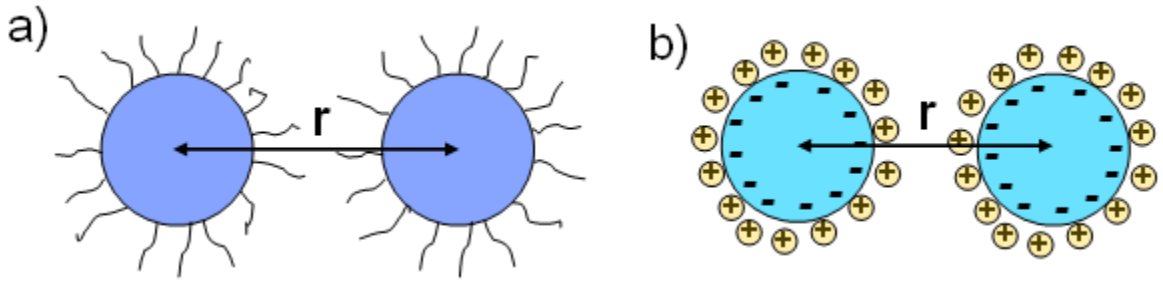

Figure 1: Stabilization methods for colloidal suspensions. a) Sterically stabilization ('hard spheres'). b) Electrostatic stabilization ('soft spheres'). Where r is the center-to-center particle distance [1].

Hard spherical particles are sterically stabilized, where the particles are chemically or physically coated with absorbing polymers or are dispersed in a non-adsorbing polymer bath. When two sterically stabilized particles come too close to each other, the polymer chains are compressed which nearly leads to a repulsive force between these. Electrostatic stabilization leads to a soft sphere colloidal suspension [see on fig 1]. Some of the soft systems consists of crosslinked, polymeric particles with sophisticated repulsive interaction potentials. Since some of these systems can be squeezed, a nominal volume fraction, ϕ, based on particle size and their number concentration is defined. For deformable soft spheres, the main difference to hard sphere systems is that the particles can be squeezed which leads to sophisticated interparticle potentials.

The main order parameter for a colloidal hard sphere system is the particle concentration, expressed as the volume fraction [2]. The volume fraction has the form

$$\phi = \frac{4}{3}\pi R^3 \rho \qquad (1)$$

Where R is the particle radius and $\rho = \frac{N}{V}$ is the number density, the ratio between the number of particles N and the sample volume V.

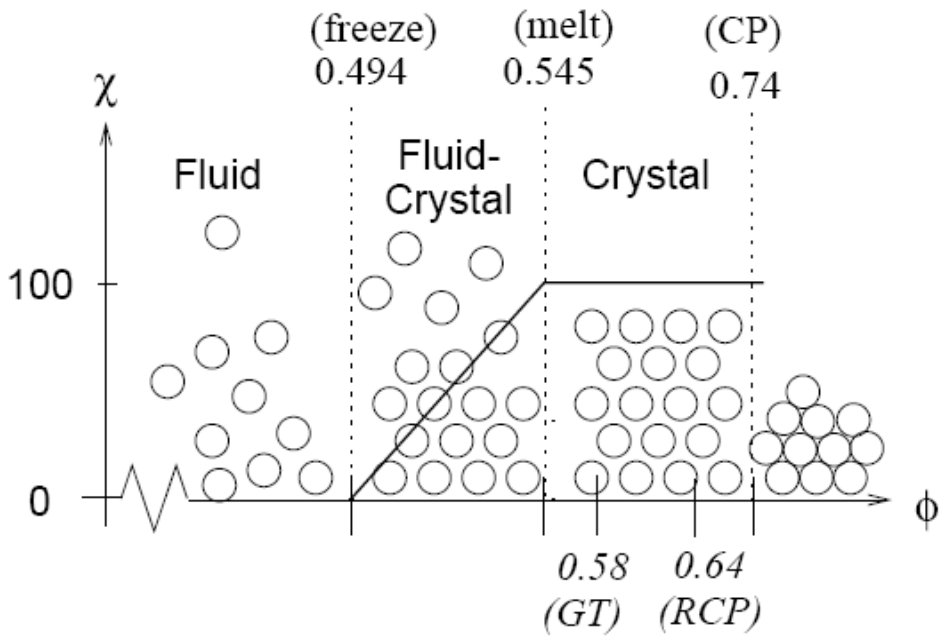

Figure 2: Phase diagram for a colloidal hard sphere system. X is the degree of crystallization while ϕ is the volume fraction [1]. (GT Glass transition, RCP Random Closed Packing)

The crystallization progress X (in percent) is plotted as a function of volume fraction [figure 2]. The (stabilized) system is in the liquid phase for low volume fractions $\phi < 0.494$. Increasing the particle concentration results in a colloidal fluid/crystal coexistence ($0.494 < \phi < 0.545$), so that small crystallites are observed. Further increase of the volume fraction leads to a complete crystallization of the colloidal system. If the particles are randomly arranged then the volume fraction is given by the random closed packed value of $\phi_{rcp} = 0.64$. The theoretical close packing value for spheres is given by $\phi_{CP}=0.74$.

2.2 Synthesis of monodispered Silica

The Stöber synthesis is a process for the preparation of monodispersed particles of silica [3]. The synthesis process of silica particles was discovered in 1968 by Werner Stöber , and based on an earlier work by Kolbe published 1956. Since then the topic has been widely studied [2].
This synthesis process has been developed to controll growth of spherical silica particles of uniform size by means of hydrolysis of alkyl silicates and subsequent condensation of silicic acid in alcoholic solutions. Ammonia is here used as a morphological catalyst [3].
For the preparation tetraethyl ortho-silicate (TEOS) is added to a low molar-mass alcohol- such as ethanol- and ammonia. The solution is then stirred. Silica particles are formed with diameters between 50 and 2000 nanometers. The size depends on the type of silicate ester used, the alcohol used and the volume ratios of each component.

2.3 Poly-N-isopropylacrylamide (pNipam)

One of the most popular soft systems are aqueous dispersions of Poly-N-isopropylacrylamid (pNipam) nanogels.
The molecular structure of pNipam (–(-$CH_2CHCONH_2$-)n-) is presented in figure 3:

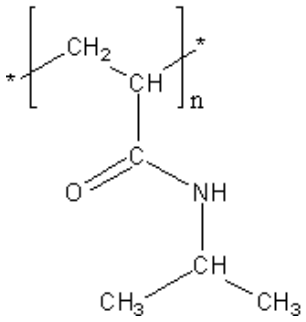

Figure 3: Schematic structure of molecular pNipam

Aqueous dispersion of microscopic size of Poly-N-isopropylacrylamid (pNipam) nanogels consist of thermosensitive polymeric particles which are dispersed in destilled water [1].
PNipam is a soft nanogel which shows a temperature responsive behavior with a sudden collapse in particle size at 32°C known as volume phase transition temperature (VPTT) due to the large volume change during the transition [see on figure 4 and 5]. Below the VPTT the particles are swollen (they are hydrophilic) and therefore show a high permeability so that the chemical potential as well as the refractive index of water is equal inside and outside the nanogel particle. While the particles collapse the permeability suddenly decreases and the refractive index and chemical potential inside the particle changes to that of the linear polymer chain [1, 7].

Thermosensitive microgels made of N-isopropylacrylamide (Nipam) crosslinked with N,N-methylenebisacrylamide (BIS) are well-studied systems. Due to the change in size induced by external stimuli such as temperature, pH and ionic strength these colloidal particles belong to the group of so-called smart materials. They combine properties of classical colloids (e.g. crystallization) with the properties of a responsive polymer system. The swelling behavior of the polymer network inside microgels made of Nipam can be described by the classical Flory–Rehner theory. It describes the equilibrium swelling of a lightly crosslinked polymer in terms of crosslink density and the quality of the solvent. With respect to the formation of colloidal crystals all poly(N-isopropylacrylamide), pNipam, microgels behave slightly differently compared to classic hard-sphere colloids like for example, poly(methyl methacrylate), PMMA, latex particles or silica nanoparticles. Due to the strong change of particle volume close to the lower critical solution temperature (LCST) of the polymer, colloidal crystals of thermoresponsive microgels can melt. This phenomenon might be exploited to reduce the number of grain boundaries in the obtained opal structure. These microgels have interesting additional properties compared to pure pNipam particles. It was, for example, shown that they are useful to control the catalytic activity of silver nanoparticles [6, 8].

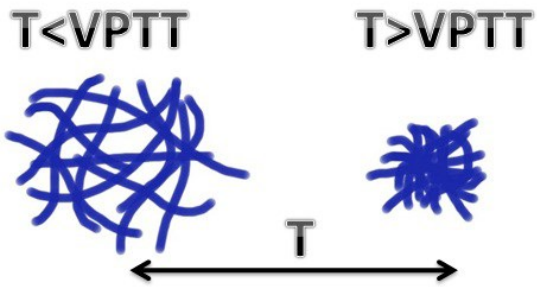

Figure 4: Particle size of PNiPAM dependent of temperature. Swollen particle (left), collapsed particle (right) [1].

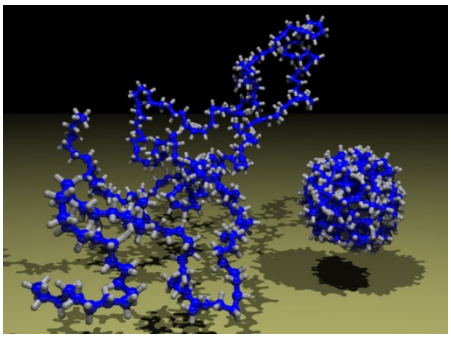

Figure 5: Swollen particle (left), collapsed particle (right).

Interestingly pNipam dispersions exist in three phases (liquid, crystal and glass phase). In figure 6 is shown that each phase can be obtained by changing weight-percent or the temperature.

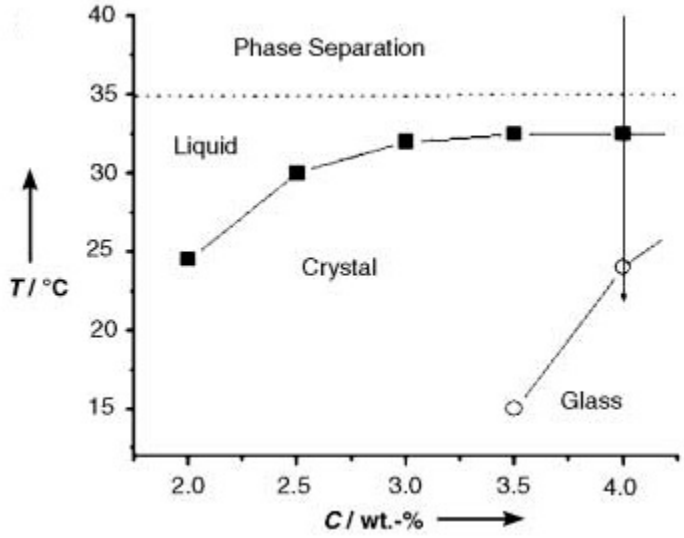

Figure 6: Phase diagram of aqueous pNipam solution taken from [4].

In the diagram the glass-transition line is indicated by the open circles, and the melting occurred by the filled black squares. One can see that at a fixed weight-percent (> 4 wt. %) it is possible to transfer the pNipam system from the glassy over the crystalline towards the liquid phase just by

increasing the temperature. Due to the crosslinker used in the synthesis, the PNiPAM particle sizing is reversible.

In general it is possible to bond the polymer chains chemically or physically.
The chemical cross-linker N-N-Methylenenbisacrylamide was used to ensure that the particle size is reversible during heating/cooling. Furthermore, the pNipam particles are weakly charged which stabilized the particles in the dispersions.

a) N, N'-Methylenebisacrylamide

N, N'-Methylenebisacrylamide (BIS) is a cross-linking agent used during the formation of polymers such as polyacrylamide. Its molecular formula is $C_7H_{10}N_2O_2$. Bisacrylamide is used in biochemistry as it is one of the compounds of the polyacrylamide gel (used for SDS-PAGE).
N,N'-Methylenebisacrylamide polymerizes with acrylamide and is capable of creating cross-links between polyacrylamide chains, thus creating a network of polyacrylamide rather than unconnected linear chains of polyacrylamide. The two double bonds present at the either ends are responsible for crosslinkage with the acrylamide.

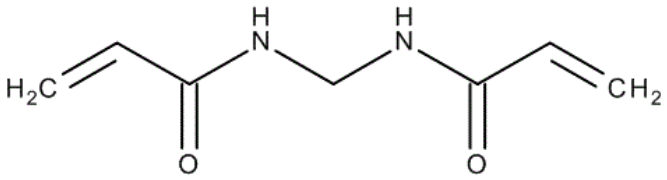

Figure 7: Schematic structure of molecular N, N'-Methylenebisacrylamide

b) Sodium dodecyl sulfate

Molecular structure $C_{12}H_{25}NaO_4S$

This is the surfactant. This forms micelles and within the micelles the Nipam monomer and are dispersalable. Surfactant stabilizes the monomer and then the polymer chain grows in the micelles.

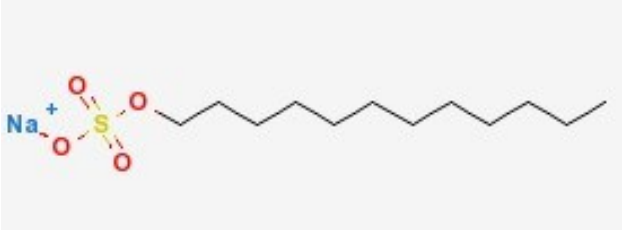

Figure 8: Chemical Structure of sodium dodecyl sulfate

c) Potasium peroxodisulfate

Molecular structure $K_2O_8S_2$

It is the initiator. It decomposes and forms the radical initiator.

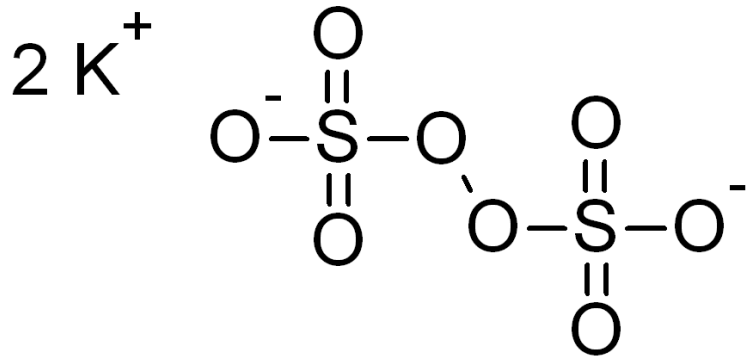

Figure 9: Chemical Structure of Potasium peroxodisulfate

2.4 The polymerization of SiO_2/pNipam

Hybrid particles attracted scientific interest due to the possibility of combining different properties in individual particles with different compositions. These particles are commonly defined by a core-shell structure. The core often responds to an external field whereas the shell stabilizes the core, makes it compatible with the environment and provides additional responsive properties. Many interesting technological applications can be foreseen for these materials, including separation technology, catalysis (nanoreactors), biochemistry (conjugates of quantum dots and antibody), medicine (drug targeted delivery), etc.

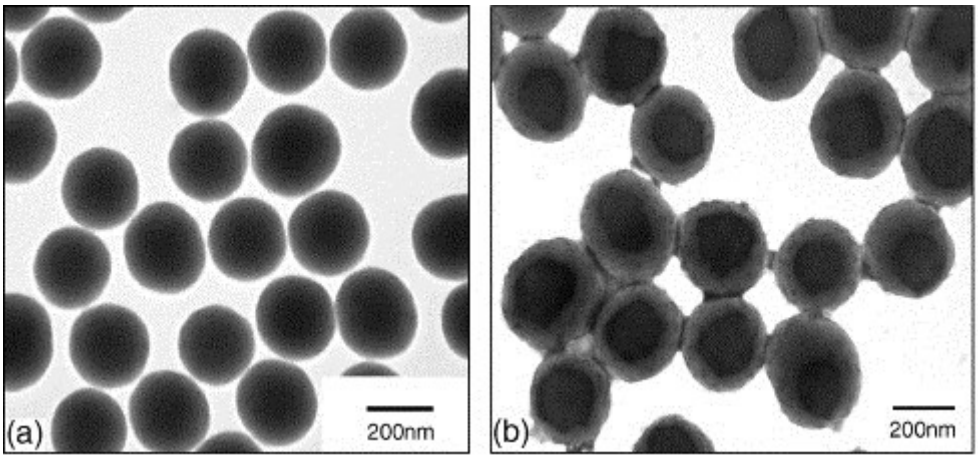

Figure 10: Transmission electron microscope (TEM) images of initiator-modified (a) and PNIPAM modified (b) silica nanoparticles [3]

A thermoresponsive hydrogel with a silica core was synthesized by aqueous surface-initiated atom transfer radical polymerization at room temperature. They owned clear core/shell structures and showed good thermoresponsiveness. Furthermore, the lower critical solution temperature LCST of pNipam is 32 °C and it approaches to the body temperature of human beings, so these thermoresponsive silica nanoparticle/pNipam (core-shell) hybrid particles must be widely used in the future[8].

Silica/pNipam core-shell system particle were prepared by a three step synthesis. The silica particles, which were firstly synthesized by the Stöber method, were used as the templating cores [2, 3].

In order to encapsulate such silica particles fully by radical polymerization, they were modified with 3-Trimethoxysilylpropylmethacrylate (TPM), leading to formation of terminal double bonds (C═C) at the core particle surface, which can produce covalent bonds between the inorganic substrate and an organic moiety.
NIPAM was polymerized with a crosslinker of N,N-methylenebisacrylamide (BIS) in the presence of the modified silica particles as seeds, resulting in formation of silica/crosslinked pNipam core/shell composite particles.
The third step is a radical emulsion polymerization.

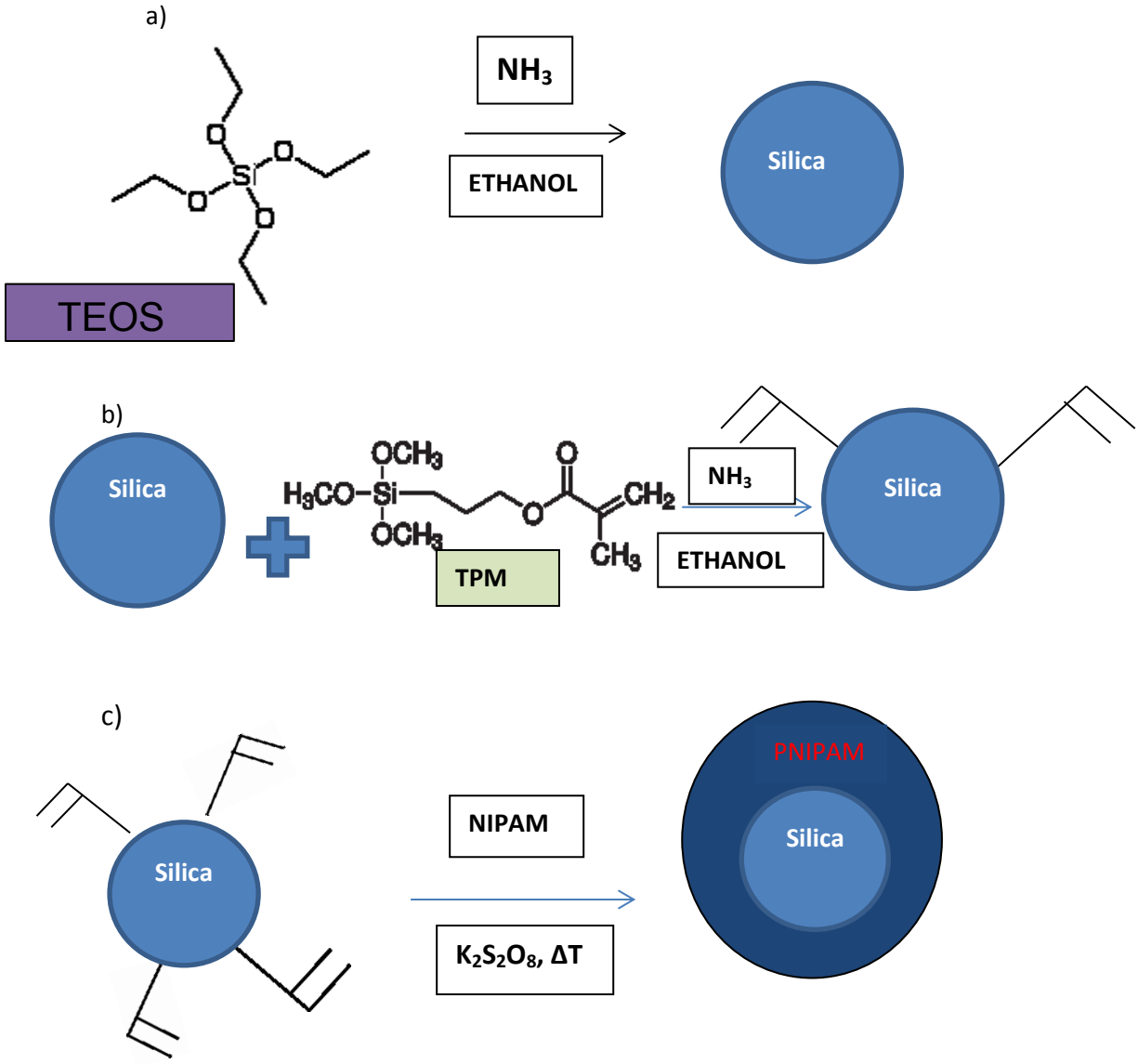

Figure 11: The polymerization of Si02/pNipam a) Stöber synthesis b) The polymerization of Si02/pNipam c) Radical Emulsion polymerization of Nipam around Silica/TPM

2.5 Emulsion polymerization

Emulsion polymerization is a type of radical polymerization that usually starts with an emulsion incorporating water, monomer, and surfactant. The most common type of emulsion polymerization is an oil-in-water emulsion, in which droplets of monomer (the oil) are emulsified (with surfactants) in a continuous phase of water.

Advantages of emulsion polymerization include:

- High molecular weight polymers can be made at fast polymerization rates. By contrast, in bulk and solution free radical polymerization, there is a tradeoff between molecular weight and polymerization rate.
- The continuous water phase is an excellent conductor of heat and allows the heat to be removed from the system, allowing many reaction methods to increase their rate.
- Since polymer molecules are contained within the particles, the viscosity of the reaction medium remains close to that of water and is not dependent on molecular weight.
- The final product can be used as is and does not generally need to be altered or processed.

Disadvantages of emulsion polymerization include:

- ✓ Surfactants and other polymerization adjuvants remain in the polymer or are difficult to remove
- ✓ For dry (isolated) polymers, water removal is an energy-intensive process
- ✓ Emulsion polymerizations are usually designed to operate at high conversion of monomer to polymer. This can result in significant chain transfer to polymer.
- ✓ Can not be used for condensation, ionic or Ziegler-Natta polymerization, although some exceptions are known.

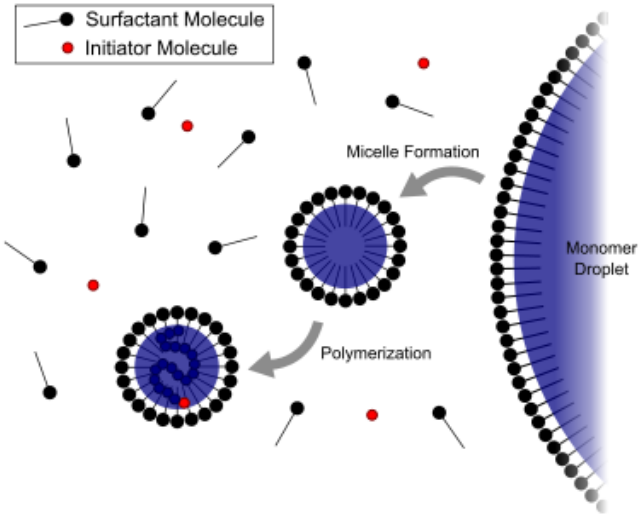

Figure 12: Schematic diagram of emulsion polymerization [11]

A monomer is dispersed or emulsified in a solution of surfactant and water forming relatively large droplets of monomer in water. Micelles are created in the water because of excess surfactant. Small amounts of monomer diffuse to the micelle through the water. The initiator reacts with the monomer in the micelles and inside the micelles polymer chain are growing. The total surface area of the micelles is much greater than the total surface area of the few, larger monomer droplets. The monomer in the micelle quickly polymerizes and the growing chain terminates. At this point the monomer-swollen micelle has turned into a polymer particle. More monomer from the droplets diffuses to the growing particle, where more initiators will eventually react. Eventually the free monomer droplets disappear and all remaining monomer is located in the particles. The final product is a dispersion of polymer particles in water (it can also be known as a polymer colloid) [11].

3 Theory of the Light Scattering Methods

3.1 Dynamic Light Scattering [1, 5]

The Dynamic Light Scattering is a technique, which measures the time-dependent fluctuations in the intensity of scattered light which occurs because the particles are undergoing random, Brownian motion [see Fig 14 left]. Analysis of these intensity fluctuations enables the determination of the distribution of diffusion coefficients of the particles, which gives access to the size distribution.

The upper size limit of the Dynamic Light Scattering is sample density dependent; as dynamic light scattering requires that particles are randomly diffusing, the upper size limit is placed as the point where sedimentation of the particle starts to dominate the diffusion process. The lower size limit of Dynamic Light Scattering depends upon the excess scattered light the sample generates compared to the suspending medium. Many factors contribute to this lower size limit including the sample concentration, the relative refractive index i.e. the particle refractive index compared to the medium refractive index, laser power, laser wavelength, sensitivity of the detector and optical of the medica configuration of the instrument. The lowest particle size measured on an instrument containing non-invasive backscatter (NIBS) is 0.6 nanometers [1].

Since the particles in diluted samples (non-interaction particles) are undergoing constant Brownian motion we are dealing with quasi-elastic light scattering. The wave vectors of the incoming and scattering light are accordingly equal: $|k_{out}| = |k_{in}|$ (see Fig.13).

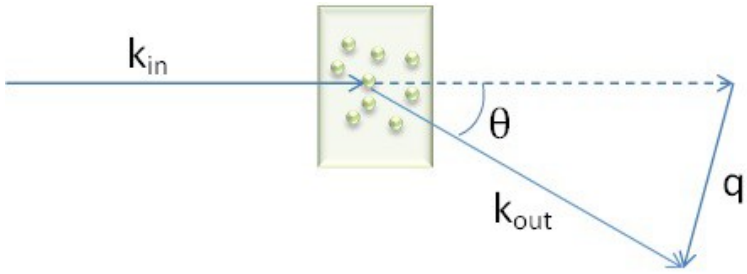

Figure 13: Schema of the scattering geometry [1]

q is the scattering vector and is defined as:

$$q = k_{out} - k_{in} \tag{2}$$

$$q = \frac{4\pi n_0}{\lambda} \sin\left(\frac{\theta}{2}\right) \tag{3}$$

Where n is the refractive index of the solution, θ is scattering angle, λ is the wavelength of the light. In order to determine the diffusion coefficient one needs to know the field-field autocorrelation $g_1(q,\tau)$ function given by

$$g_1(q,\tau) = \frac{<E_S(t)E_S^*(t+\tau)>}{<|E_S(t)|^2>} \tag{4}$$

Where <> denotes time averaging, τ is the lag time.
The experimental measurement of the field-field correlation function is not possible and so one needs to measure the intensity-intensity correlation function $g_2(q,\tau)$ given by equation below

$$g_2(q,\tau) = \frac{<I(t)I_S^*(t+\tau)>}{<|I_S(t)|^2>} \quad (5)$$

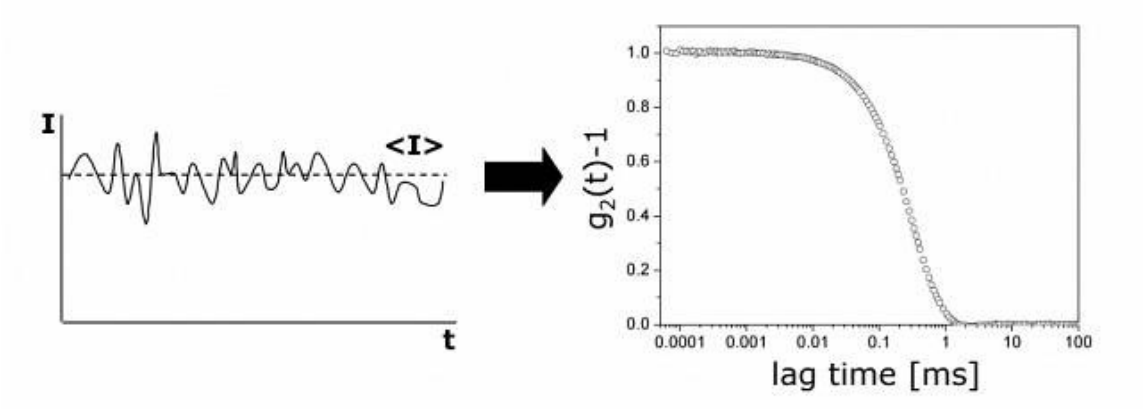

Figure 14: Intensity of scattered light from an aqueous solution as a function of time (left), Correlation function shows the dependence relation g_2 to time(right) [9]

The intensity-intensity correlation function [see on Fig 14 (right)] is related with the field-field correlation function by the Siegert's relation given by the following equation.

$$g_2 = 1 + \beta|g_1(q,\tau)|^2 \quad (6)$$

where β is the coherence factor, which depends on the instrumental set-up like the detector optics. Conventional laser light shows a nearly perfect coherence with β~1.
From the intensity-intensity correlation function one can extract the field-field correlation function using equation (4). The field-field auto correlation function is related to the decay rate (Γ) by

$$g_1(q,\tau) = \exp(-\Gamma\tau). \quad (7)$$

The decay rate, Γ is proportional to the diffusion coefficient

$$\Gamma = q^2 D_t\,. \quad (8)$$

From the diffusion coefficient D it is possible to determine the hydrodynamic radius of the particles by using Stokes-Einstein relation given by

$$D = \frac{k_B T}{6\pi\eta R_H} \quad (9)$$

where k_B is the Boltzmann constant, η is the solvent viscosity and R_H is the hydrodynamic radius of the particle, T is the temperature and D is the diffusion coefficient.

The correlation of the intensity (see Fig. 14) can be performed by electronic hardware or software analysis of the photon statistics. Because fluctuation is typically in the range of nanoseconds to milliseconds, electronic hardware is typically faster and more reliable at this job.

4 Experimental setup and material section

4.1 Light scattering setup

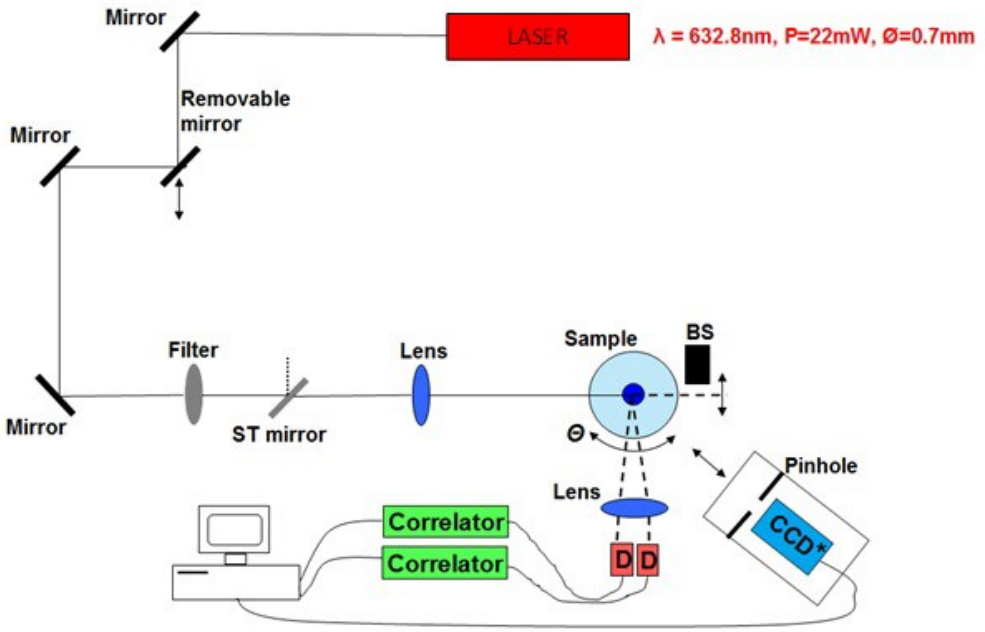

Figure 15: Schematic setup to the experimental of the light scattering [1]

This experiment used a 3D DLS spectrometer from LS instruments [see fig. 15]. Two avalanche photodiodes (APDs) were fixed on the goniometer arm. The goniometer arm can be placed between 20° and 150° scattering angle. The extended setup consists on the light source that is represented by the He-Ne laser [1].

The typical parameter of the HE-NE laser are listed above

- Wavelength λ=632.8 nm
- Power P ($TEM_0 0$) 22 mW
- Beam diameter ($1/e^2$) 0,7 mm
- Beam divergence 1.15 mrad
- Polarization ratio 500:1 (vertical)

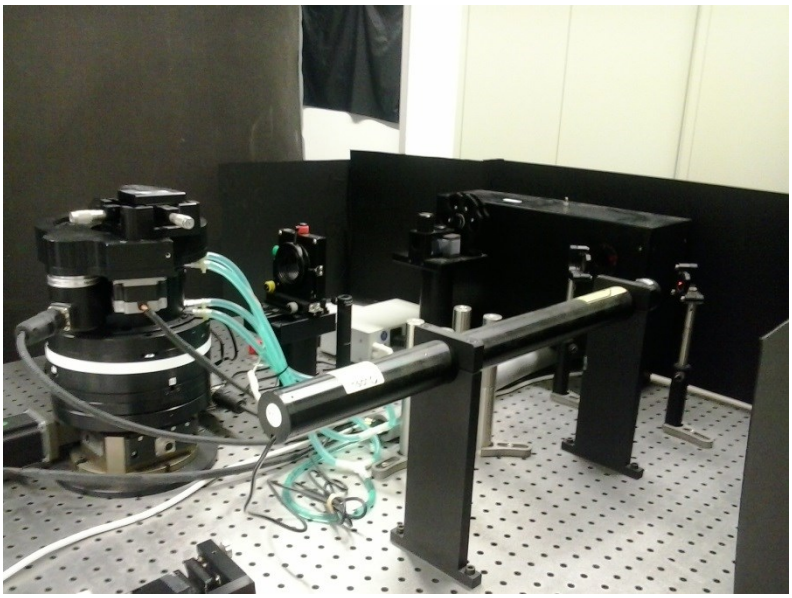

Figure 16: Photo of the setup to the light scattering

Before the beam from He-Ne laser reaches the filter systems it has deflected two times. These filter systems are mounted very close to the laser head due to the high laser power. The laser light is focused by lens into the sample cell and the signal of the scattered light can be measured by APDs. To overcome parasitic scattering of the sample cell wall, the samples are placed in a cis/trans-decalin bath, whose the refractive index is close to all substances used in the experiment, and therefore minimizes the deviation due to refraction. The temperature is controlled by a Julabo water refrigerated/heating circulator (Julabo Labortechnik GmbH, Seelbach / Germany) which is connected with the decalin bath. The APDs are used to measure the hydrodynamic radius of the diluted pNipam samples [1].

4.2 Materials

4.2.1 Recipes for Silica Particles by Stöber synthesis

Synthesis of the core particle modified with TPM

Table 1: Amounts of the substances needed for the synthesis of Silica particles

Substances	Used Volume (ml)
Tetraethyl orthosilicate (98%) $Si(OC_2H_5)_4$ TEOS:	5 ml
Ammonium hydroxide NH_4OH (25%):	15 ml
Ethanol (99%) EtOH:	200ml
3-Trimethoxysilylpropylmethacrylate (98%) $Si(OC_2H_5)_5$: 1 ml	

The ammonium hydroxide is put to ethanol solution in a beaker (or Erlenmeyer flask). Then the TEOS is added all at once. The reaction mixture is then stirred with magnetic stirrer with a reaction speed of about 500-600-rotation/ minutes for 12 hours at room temperature. Then 10 ml of ammonia and 1 ml of 3-Trimethoxysilylpropylmethacrylate (TPM) all is added and the reaction mixtures is stirred for further 24 hours. The next day the mixture is filtered and the ethanol and ammonia are evaporated in a vacuum evaporator (the pressure is set to 170 mbar and the water bath temperature to 40°C).

4.2.2 Synthesis Poly(N-isopropylacrylamide)/Silica Gel Hybrid (Synthesis of the shell)

Table 2: Amounts of the substance needed for the synthesis (Sample 5)

Substances	Molecular formula	Needed Weight [g]
Silica gel SiO_2		all of the silica particles are taken from the synthesis
Sodium dodecyl sulfate (SDS)	$C_{12}H_{25}NaO_4S$	(0.378g)
Sodium sulfite anhydrous	Na_2O_3S	(0.567g)
N-isopropylacrylamide monomer (NiPAM)	$C_6H_{11}NO$	(10 g)
N-N-Methylenenbisacrylamide	$C_7H_{10}N_2O$	(0.44g)
Potasium peroxodisulfate	$K_2O_8S_2$	(0.405g)
Ammonium- iron (II) sulfate Hexyhydrate	$FeH_8N_2O_8S_2$	(1 crystal)
Deionized water		Till 1500 mL

In a 2.5 L three-neck flask the silica/TPM solution in ethanol was mixed with sodium dodecyl sulfate, sodium sulfite anhydrous, half of the monomer (Nipam), and half of N-N-Methylenenbisacrylamide and with deionized water. All of these substances were weight with a precision balance (precision of 0.0001 g). For the exact amounts see the table 2 above.
The magnetic stirring was used in order to dissolve all the substances in the water. Before initiating the reaction, a nitrogen supply was connected to the three necked flask to remove present oxygen in the reaction mixture from evaporating. The mixture was heated to 60 °C. In between the potassium peroxidisulfate was dissolved 10 ml of water. After one hour the potassium peroxidisulfate was added to the reaction mixture together with a crystal of ammonium- iron (II) sulfate to initialize the polymerization. The ammonium-iron (II)-sulfate and the sodium sulfit reacts as a redox system, that the reaction can already start at 60°C.
After another hour the rest of the monomer (Nipam) and the crosslinker N-N-Methylenenbisacrylamide are added. The reaction is ongoing for the next six hours. To stop the reaction the nitrogen flux was stopped and the heating was turned off.The solution was stirred until the next day. Then the dispersion was filtered in order to remove impurities. After that it was placed inside a dialysis membrane and dialyzed against deionized water. The deionized water was changed twice per day to accelerate the process.
One week later the dialyzed particle dispersion was reconcentrated several times in a rotating evaporation assembly. This was accomplished by use of a warm water bath and a pressure reduction by a vacuum pump (80-100 mbar) by measuring concentrations of the samples before and after evaporating the water on it in a vacuum oven. The weight percent was calculate via:

$$wt\% = \frac{m_a - m_e}{m_b - m_e} \cdot 100\% \quad (10)$$

where m_a is weight of the sample before evaporation
m_b is weight of the sample after evaporation
m_e is tara's weight

4.2.3 Synthesis Silicia/pnipam (Sample 6a/e-five shells of pNipam)

Table 3: Amounts of the substance needed for the synthesis

Substances	Needed Weight [g]
Silica/TPM (SiO_2) in ethanol	all of the silica particles are taken from the synthesis
Sodium dodecyl sulfate (SDS)	(0.378g)
Sodium sulfite anhydrous	(0.417g)
N-isopropylacrylamide monomer (NiPAM)	(2 g)
N-N-Methylenenbisacrylamide	(0.088g)
Potasium peroxodisulfate	(0.405g)
Ammonium- iron (II) sulfate Hexyhydrate	(1 crystal)
Deionized water	Till 1500 mL

Samples 6a was prepared as the same way as the sample above. The next day 400 mL of dispersion was casted and filtered in order to remove impurities. After that it was placed inside dialysis membrane and dialyzed against deionized water.

Table 4: Amounts of the substance needed for the synthesis

Substances	Needed Weight [g]
N-N-Methylenenbisacrylamide	(0.1g)
Sodium sulfite anhydrous	(0.208g)
N-isopropylacrylamide monomer (NiPAM)	(2 g)
Deionized water	400 mL
Potasium peroxodisulfate	(0.202g)
Ammonium- iron (II) sulfate Hexyhydrate	(1 crystal)

The synthesis samples 6b-6e was repeated 4 times because we wanted to get next shell of pNipam. After each synthesis a portion of dispersion was put into the membrane.
In this way five samples were received, which have the same size of core (silica particle) and different size of shell (pNipam).

4.2.4 The sample 3 and 4 have been prepared already beforehand.

Weight fraction
Sample 3: 3.76 wt%
Sample 4: 6.24 wt%

5. Results

In this section the results of the experiments are presented. It is divided into three different parts. First we will present the result for the core particles consisting of silicium oxide. In the next section we will discuss the results for the silica/pNipam core-shell particles consisting of a silica core and a pNipam shell. We will observe that the silica/pNipam core shell particles have the same thermoresponsive behavior like pNipam itself. In the third section we will show the results of different thicknesses of the pNipam shell.

5.1 Silica core

After the preparation of the silicium oxide core modified with TPM, a small amount of the sample was separated for characterization. For the dynamic light scattering a diluted sample with ethanol was prepared. The dispersion must be almost colorless to avoid any multiple scattering. Even though the dynamic light scattering is a remarkable technique for characterization it is very sensitive to dust and hence extra care has to be taken during sample preparation.

Since the size of silica particles does not change under the influence of temperature, the particles are used as a control sample. After covering with pNipam we expect to see a change of the particle size in the collapsed state, i.e. at high temperature. To determine the size of the silica particles the autocorrelation function g_2 (q,t) of the intensity (eq. 5) was measured for different q-values. The scattering angle was set between 40°-120°. The exact angle and temperature was read out directly by the DLS software. Each angle has been measured for 120 s. Here we plot g_2 (q,t)-1 of the colloidal silica particles suspended in ethanol for different wave vector is q (Fig. 17). The wave vector q was calculated via eq. 3. For better reading we shifted the curves horizontally. For short time scales the particles motion is correlated and the dynamical structure factor is constant. For long time scales the particles get completely decorrelated and the autocorrelation function drops exponentially to the baseline. With increasing wave vector q, the relaxation time τ is decreasing, which is visible by a shift of the exponential decay to shorter timescales. The relaxation rate Γ (=1/ τ) has then been extracted via a fit of the dynamical structure factor to the autocorrelation function using the Siegert relation (eq. 6) and a single exponential fitting function (eq. 7).

The relaxation rate Γ is proportional to the square of the wave vector q (Fig. 18), which is a typical behavior for Brownian motion (eq. 8). To calculate the size of the silica particles the Stokes-Einstein relation was used (eq. 9). The sample was measured at a temperature T = 20°C. The silica particles have a hydrodynamic radius of about R_h = 67 nm. This core particle was used for the preparation of the core shell system Si/pNipam 05.

The silica particles for the core shell system Si/pNipam 06 had a particle radius of about 63 nm.

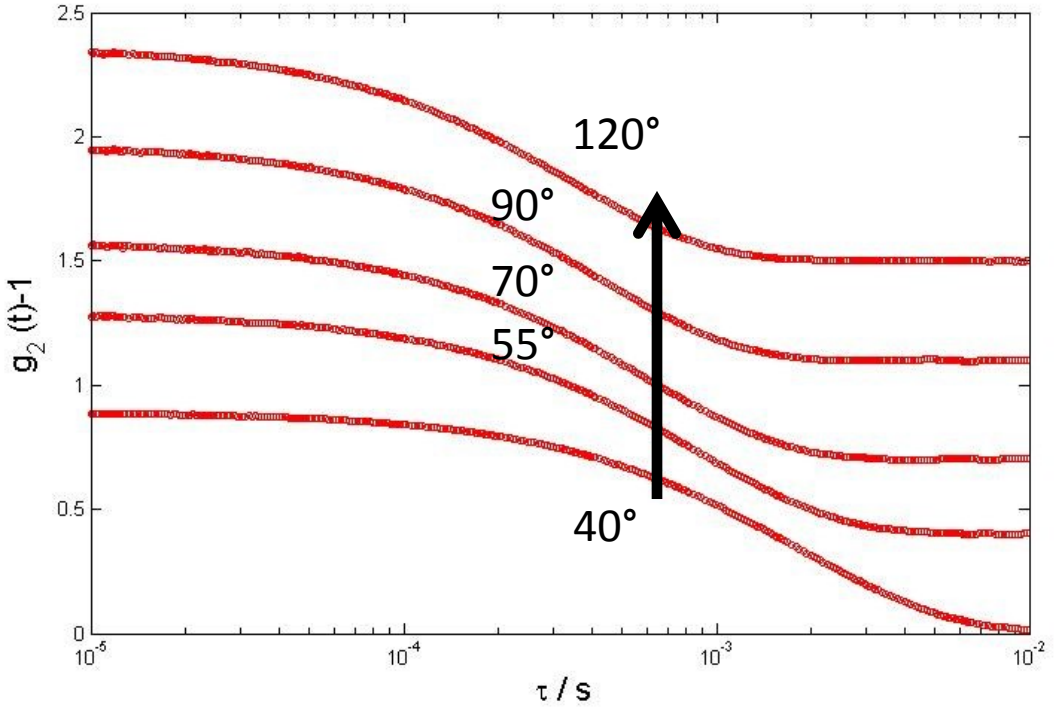

Figure 17: Auto-correlation function of the intensity for different q-values measured for the silica core particles in ethanol.
correlation functions are shifted for better readability..

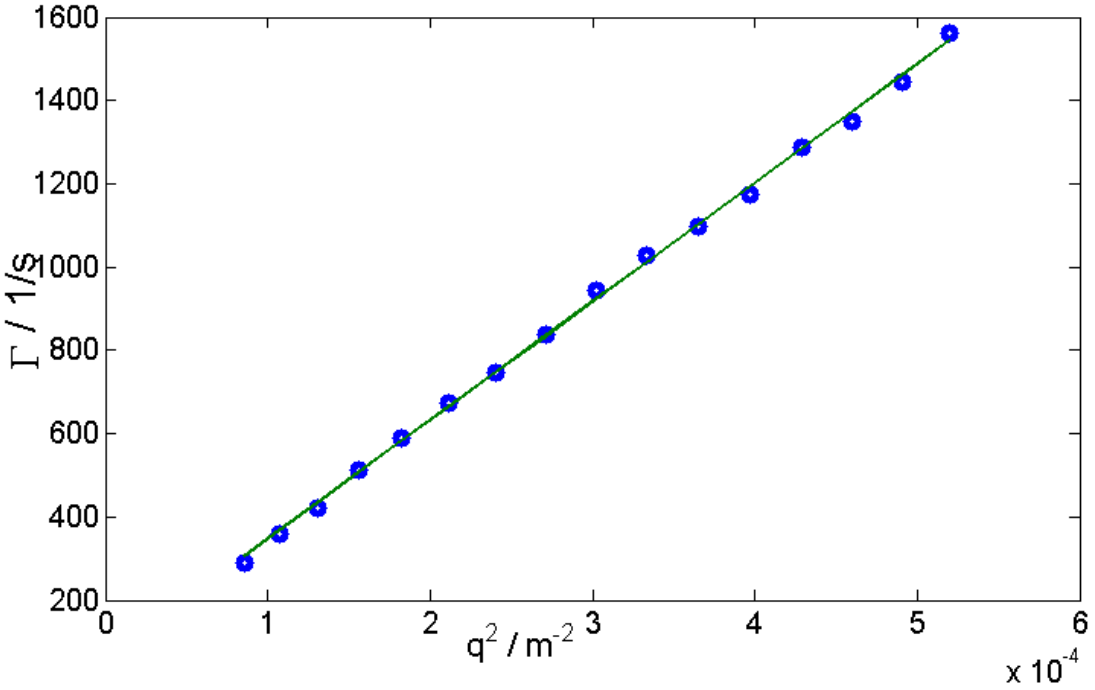

Figure 18: Extracted relaxation rate Γ correlation function for the silica particles in ethanol (core particles for Si/pNipam 5) plotted vs. the square of the wave vector q.

5.2 Core shell system

In opposite to the silica particles pNipam changes the particles hydrodynamic radius where changing the temperatures. Therefore the silica/pNipam core shell system is measured at different temperature in the same way like described for the silica particles. In order to detect the thermo-responsive behavior (figure 19) the temperature was changed. First the temperature was set to 10°C then the temperature was stepwise increased to 48°C and then again decreased to 20°C. Before each measurement was started the temperature was stabilized for several minutes.
In figure 18 the results are displayed for a silica/pNipam core shell system (named as Si/pNnipam 5). At temperatures below 25°C the particles have a size of about 250 nm. Above 30°C there is a dramatic decrease in size. At 40°C the particles are collapsed to particles with sizes of about 162 nm and the particle size decreases at even higher temperatures.

Like pNipam the size of the core shell particles depends strongly on the temperature. The size of the silica/pNipam core-shell before and after heating is similar. Further temperature cycles show continuously reversible expansions and contractions of the core shell particles. The exact temperature for the volume phase transition for this core-shell system is not clearly visible, due to almost two different sharp transitions. This may have happened since the pNipam shell was added in two steps.

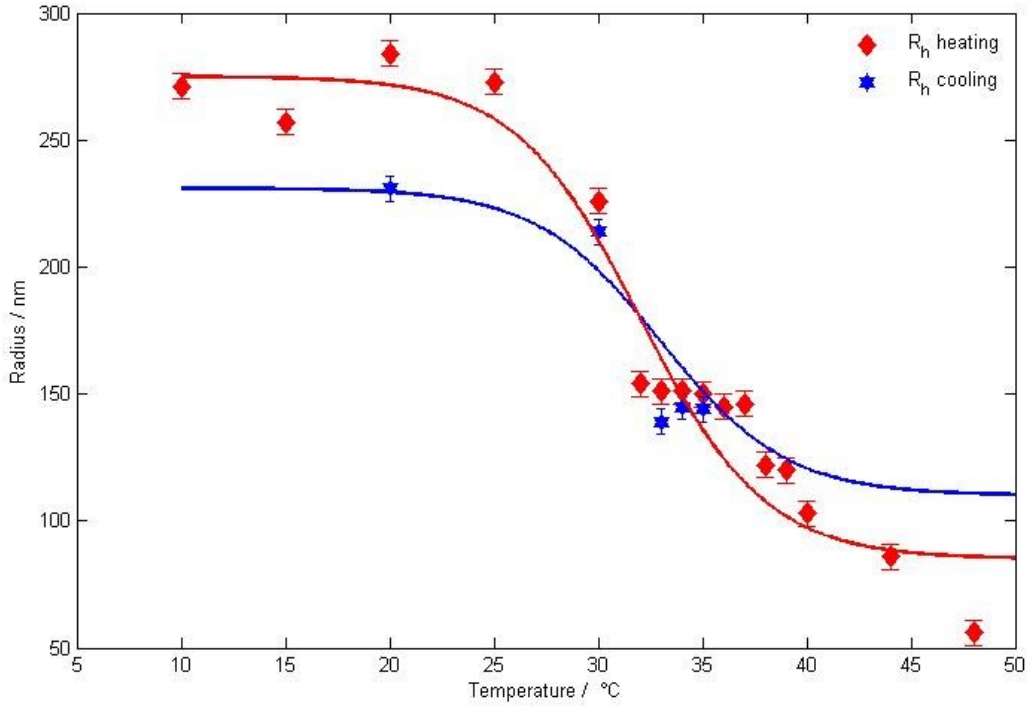

Figure19: Hydrodynamic radius of the silica-/pNipam hybrid particles determined by DLS plotted vs. the-temperature

Two more core shell systems (named as Si/pNipam 4 and Si/pNipam 5) have been investigated in the same manner. The results are shown in table 5.

The silica particles used as seed particles for Si/pNipam 5 have been measured beforehand. The comparison shows that the collapsed state can be even smaller than the hydrodynamic radius of the silica core particles used.
For the other two samples the silica core wasn't measured beforehand. Therefore no control measurement for the core particles is available.

Table 5: Measurement results of the hydrodynamic radius system core shell silica/pNipam at 40°C and at 20°C

Sample	**R_h 20°C [nm]**	**R_h 40°C [nm]**	**ΔR_h [nm]**	**Expansion coefficient (Rh)3 40°C/(Rh)3 20°C**	**Silica core [nm]**
Si/pNipam 3	285	162	123	5.4	-
Si/pNipam 4	257	103	154	15.5	-
Si/pNipam 5	214	56	158	55.8	67

5.3 Variation of the shell

In a further synthesis another silica/pNipam (named Si/pNipam 6) core shell system has been prepared. During this synthesis in five different steps, named a-e, the pNipam shell has been grown on the silica particles surface. For each shell thickness an aliquot of the sample has been taken out and measured temperature dependent by using dynamic light scattering.
In Fig. 20 the results for the different shell thickness are shown. Due to the limited time only 8 temperatures between 15 and 45 °C have been measured and the sample was not measured again at room temperature after the heating to 45°C.

For all samples at low temperature the particles are swollen.When heating a transition intro the collapsed state occurs between 30 and 35°C.

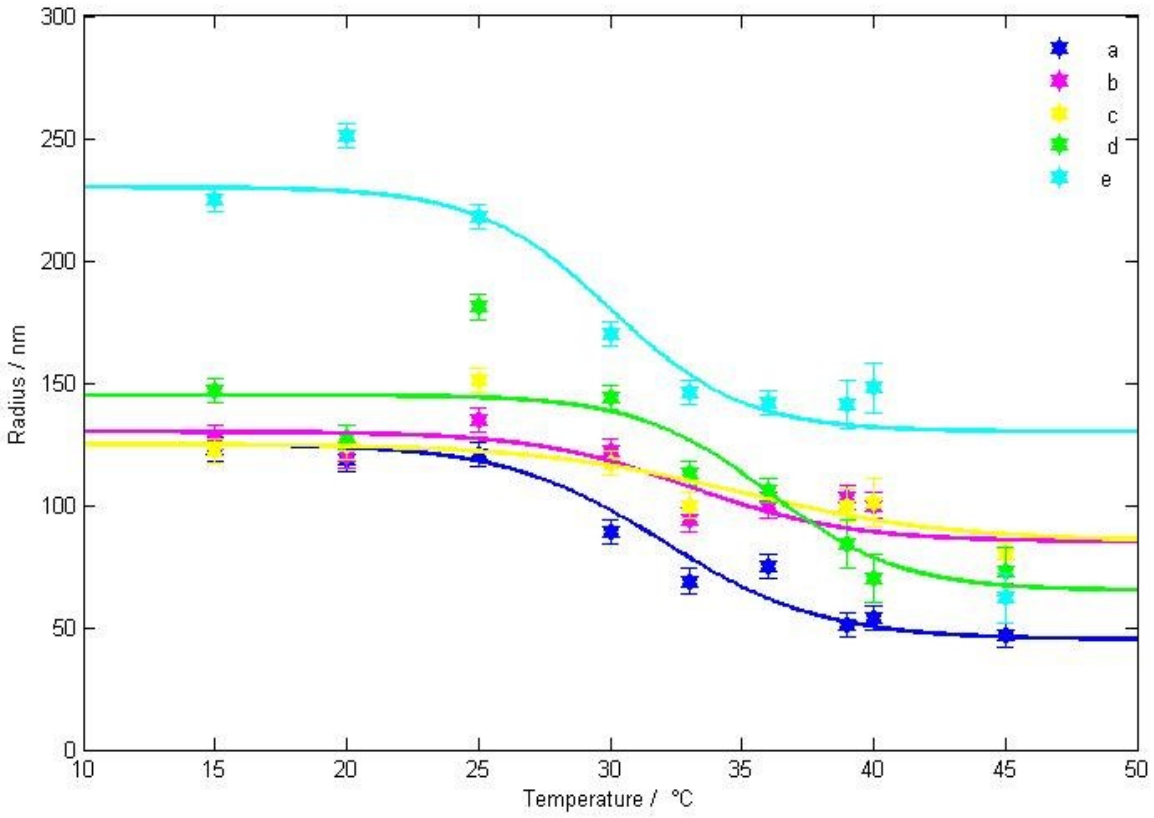

Figure 20 Hydrodynamic radius of the silica core-shell particles determined by DLS vs temperature. Sample name denote : a-first shell, b -the second shell, c –the third shell, d- the fourth shell and , e- the fifth shells. The lines are preliminary fits (eq. 11) to determine the minimal hydrodynamic radius, the maximum hydrodynamic radius as well as the transition temperature.

6. Conclusion and discussion

We successfully managed to cover the silica particles with a pNipam shell and showed that the pNipam shell exhibits a thermo-reversible behavior (see Fig. 21).

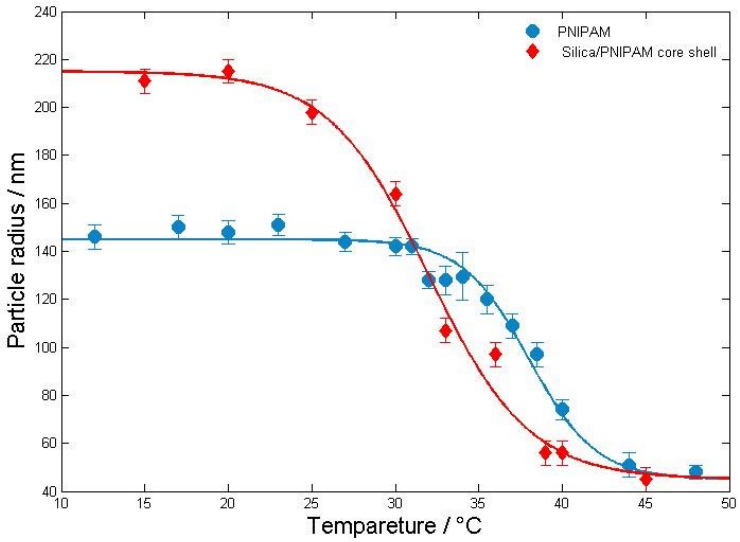

Figure 21 The plot shows the hydrodynamic radius of the pNipam and Silica/pNipam core shell for different temperature.

The plot with pNipam and the Silia/pNipam particles shows that pNipam does have the same behavior like silica pNipam core shell shows almost the same minimal radius as well maximum radius. For the synthesis we used different sizes for the silica core particles as well as different amounts of nipam. The ratio of nipam/crosslinker was kept constant.

The lines into the figures were drawn for an accurate determination of the transition temperature. The curves were fitted by Boltzmann functions;

$$R(T) = \frac{R_{H\,min} - R_{\,H\,max}}{1+\exp\left(-\frac{(T-T_{VPTT})}{dT}\right)} + R_{\,H\,max}\,. \qquad (11)$$

Where: $R_{H\,min}$is the minimal hydrodynamic radius, $R_{H\,max}$ maximal hydrodynamic radius, T_{VPTT} volume phase transition temperature and dT characterized the width of the transition [10].

From table 5 one can see that the difference between the swollen and the collapsed particle hydrodynamic radius are in all three systems Si/pNipam 3, 4 and 5 larger than 100 nm. Difference can be seen when looking at the expansion coefficient ε:

$$\varepsilon = \frac{R_h^3(LT)}{R_h^3(HT)} \qquad (12)$$

from swollen and the collapsed state. The expansion coefficient depends strongly on the size of the collapsed particles. It increases from 5.4 to 15.5 and to 55.8 with decreasing particle size of the collapsed state. We assume that this relation correspond also to the sizes of silica particles used. The three different systems show that different size of silica core particles can be used as seeds. Depending on the ratio of the shell to the core particles (and also the used amount of Nipam monomer during the synthesis) the expansion coefficient can be varied dramatically.

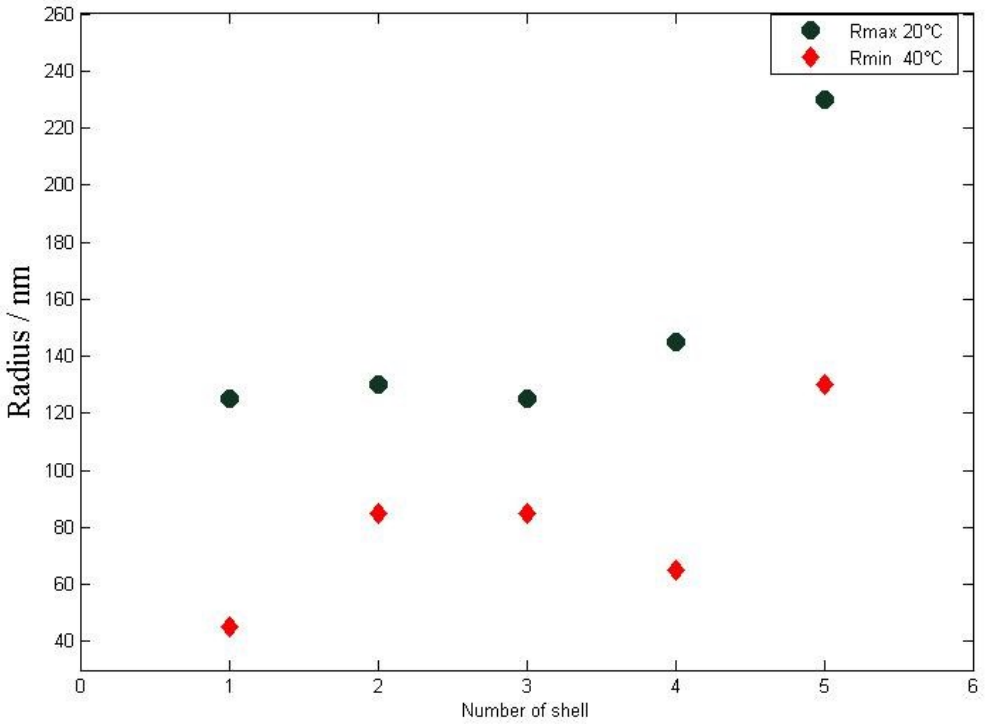

Figure 22 Hydrodynamic radius of the Si/pNipam core shell system (named Si/pNipam 6) determined by DLS shown for the different number of pNipam shells.

The hydrodynamic radius of the Silica pNipam core shell system 6 is shown for the different number of pNipam shells in figure 22. We want to note that the size of the silica core is constant. We can see that the size of the shell grows with increasing number of shells ΔR_h (Tab 6) as well for the collapsed and as for the swollen state.

Table 6: Results of measurement of the hydrodynamic radius system core- shell Silica/pNipam at 40°C and at 20°C

Sample	R_h 20°C [nm]	R_h 40°C [nm]	ΔR_h [nm]	Expansion coefficient $(R_h)^3$ 20°C/$(R_h)^3$ 40°C
Si/pNipam 6a	125	45	80	21.43
Si/pNipam 6b	130	85	45	3.58
Si/pNipam 6c	125	85	40	3.18
Si/pNipam 6d	145	65	80	11.10
Si/pNipam 6e	230	130	100	5.54

We tried to increase the shell size with the number of shells to increase the expansion coefficient. Unfortunately, the expansion coefficient is not increasing with the number of shells. The expansion coefficient is larger for one shell, and after that a significantly decrease, increase again for the fourth shell.

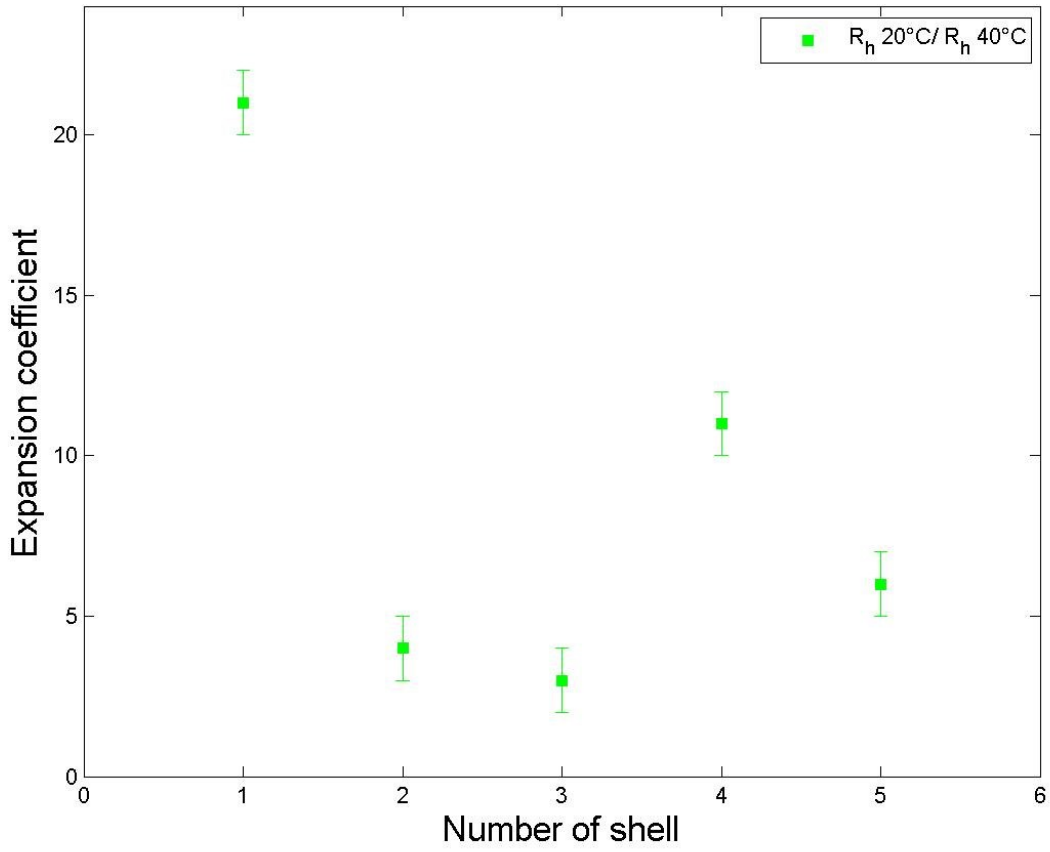

Figure 23 Expansion coefficient ε for different number of pNipam shells.

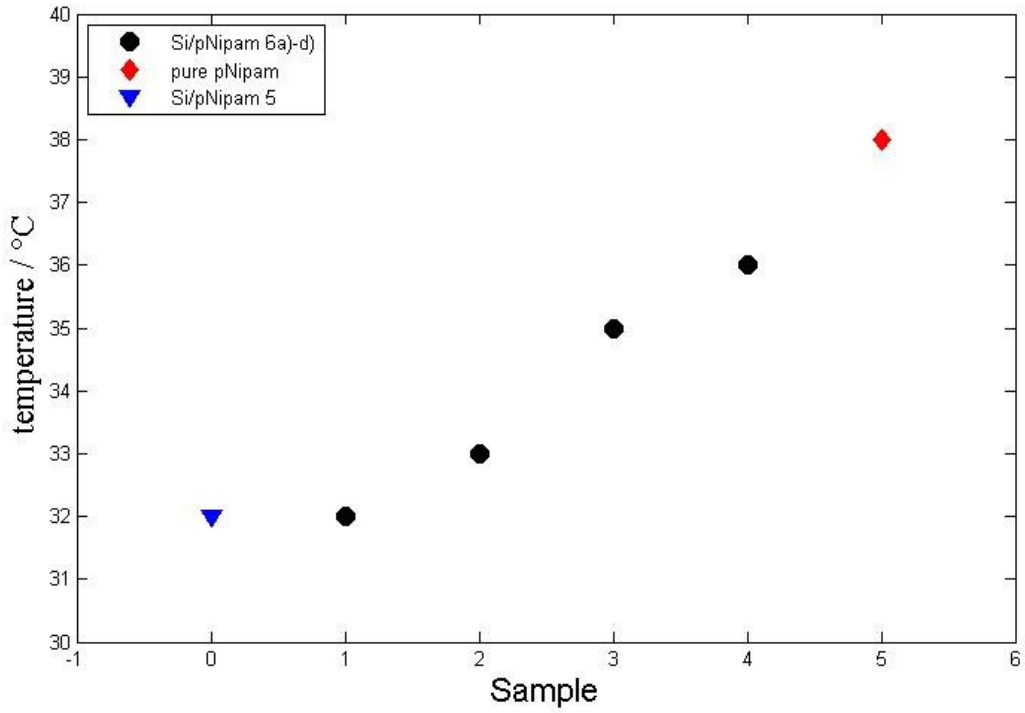

Figure 24 Plot shows the T_{VPPT} vs the number of pNipam shells.
Herein number 0 is Silica core , PNIPAM shell (only 1 synthesis step),
numbers 1-4 Silica core2, PNIPAM number of shells 1-4, pure PNIPAM particle(number5),

The different synthesis approaches adding one shell at once (Silica/pNipam 5) vs adding different shells shows that T_{VPPT} grows. Although the ratio nipam/Crosslinker is the same for each shell thetransition temperature. T_{VPPT} for pure pNipam (similar for adding more and more shells) is 38 °C and 32 °C for core-shell system.

In summary it was shown that the approach of synthesis silica/pNipam core shell particle was successful. The particle formed exhibit reversible thermoresponsive behavior like the pure microgel. These upcoming X-ray scattering measurements of this sample system allow it to investigate the structure and dynamic of colloids at high particle concentration.

References

[1]Schleitzer S. , Dynamics of Soft Nanoparticle Dispersions studied by Dynamic Light Scattering and Photon Correlation Imaging, Diploma Thesis, University of Clausthal, 2011.
[2] Ismail A.M., Ibrahim, A.A. F. Zikry, Mohamed A. Sharaf Preparation of spherical silica nanoparticles: Stober silica, Journal of American Science, Vol. 6, 985-989, 2010
[3] Stöber W. , Fink A., Controlled Growth of Monodisperse Silica Sphere in the Micron Size Range, Journal of colloid and Interface Science, Vol.26, 62-69, 1968
[4]Hu, Z. and Huang, G. A New Route to Crystalline Hydrogels, Guided by a Phase Diagram, Angew. Chem. Int. Ed. , Vol. 42, 4799-4802, 2003.
[5] Berne B., PecoraA R., Dynamic Light Scattering, with applications to Chemistry, Biology and Physics, Dover Publications, Mineola, New York, 1976.
[6] Karg M., Pastoriza-Santos I., Liz-Marzán L. M., Hellweg T., A Versatile Approach for the Preparation of Thermosensitive PNIPAM Core–Shell Microgels with Nanoparticle Cores, Chem. Phys. Chem. , Vol.7, 2298-2301, 2006
[7] Zhang K., Ma J., Zhang B., Zhao S., Li Y., Xu Y, Yu W., Wang J., Synthesis of thermoresponsive silica nanoparticle/PNIPAM hybrids by aqueous surface-initiated atom transfer radical polymerization, Materials Letters, Vol. 61, 949-952, 2007
[8] Lee Y.G., Park C. Y., Song K.H., Kim S.S., Oh S.G. , Preparation of monodispersed PNIPAm/silica composites and characterization of their thermal behaviors, Journal of Industrial and Engineering Chemistry Vol. 18 ,744–751, 2012
[9] http://www.lsinstruments.ch/technology/dynamic_light_scattering_dls/ 15.08.2013
[10] Popescu M., Filip D., Vasile C., Cruz C. Raueff J., Marcos M., Serrano J. Singurel Gh. , Characterization by Fourier Transition Infrared Spectroscopy (FT-IR) and 2D IR Correlation Spectroscopy of PAMAM Dendrimer, Journal of Physic Chemistry, Vol. 110, 14198-14211,2006
[11] http://en.wikipedia.org/wiki/Emulsion_polymerization 19.08.2013